

● Original Contribution

MEASUREMENT OF CAPILLARY PERMEABILITY  
FROM THE Gd ENHANCEMENT CURVE:  
A COMPARISON OF BOLUS AND CONSTANT  
INFUSION INJECTION METHODS

PAUL S. TOFTS\* AND BRUCE A. BERKOWITZ†

\*Institute of Neurology, Queen Square, London WC1N 3BG, UK, and

†Department of Ophthalmology, University of Texas Southwest Medical Center,  
Dallas, TX 75235-8592, USA

Dynamic imaging of Gd-DTPA uptake has been used by several groups to characterise the permeability of blood-brain barrier and blood-retina barrier lesions, using both bolus and constant infusion rate injections. However, no consensus on which injection protocol is most efficient has been reached. To address this problem, we extend our Simplified Early Enhancement (SEE) theory, applicable to retinal lesions, to cover infusion injections, and demonstrate its application to published data. The two injection methods are compared using computer simulation. We find that, first, an infusion cannot produce a constant plasma concentration in an acceptable time (although a hybrid injection, consisting of a combined bolus and infusion, is able to do this). Second, at any given time after the start of injection, a bolus achieves a higher tissue concentration, and hence enhancement, than does the same dose given as an infusion. Conversely, a bolus achieves any given tissue concentration in a shorter time than the same dose given as an infusion. Consequently, a bolus uses a smaller dose to achieve a given enhancement at a particular time. Third, if renal function is reduced, the error in calculating the permeability from a particular value of enhancement is lower for the bolus than for the infusion. And last, the SEE method is more accurate for a bolus than for an infusion. We conclude that a bolus is always more efficient than an infusion, as well as being easier to administer, and should always be used in preference to an infusion.

**Keywords:** Bolus injection; Infusion injection; Permeability; Gd-DTPA; MRI.

INTRODUCTION

Gadolinium-DTPA has been widely used to investigate abnormal leakage in the blood-brain barrier,<sup>1,2</sup> and recently in the blood-retina barrier.<sup>3</sup> In diseases such as multiple sclerosis,<sup>4,5</sup> tumours,<sup>2</sup> and retinal lesions,<sup>3</sup> Gd can leak out of the capillaries. The extent to which this happens may be an indication of the activity of the disease; alterations in the leakage could be used to investigate the natural history of the disease, including staging of tumours, and its response to therapy.<sup>6</sup> To achieve this characterisation of the leakage, a quantitative measure is needed that is precise and preferably accurate. Physiologists have characterised leaking membranes<sup>7</sup> by their permeability,  $P$  ( $\text{cm min}^{-1}$ ), defined as the flow of tracer ( $\text{mmol min}^{-1}$ ) per unit concentration difference across the membrane ( $\text{mmol cm}^{-3}$ ) and per unit surface area,  $S$ , of the membrane ( $\text{cm}^2$ ). The

total leakage in a lesion is characterised by the  $PS$  product ( $\text{cm}^3 \text{min}^{-1}$ ), defined as the product of permeability  $P$  and the surface area  $S$  of the leaking membrane (in this case the capillary bed). A third useful parameter is the  $PS$  product per unit volume of tissue, or transfer constant  $k$  ( $\text{min}^{-1}$ ).<sup>8</sup> Measurements of  $k$  can be made in vivo using MRI, and it this parameter that is considered in this paper. It will be referred to as *permeability* for brevity.

The permeability of leaking blood capillaries has been measured in the brain using a bolus injection of Gd-DTPA tracer<sup>8-12</sup> and in the retina.<sup>13,14</sup> Measured values of transfer constant  $k$  ranged from 0.0011–0.0016  $\text{min}^{-1}$  in the retina,<sup>14</sup> through 0.01–0.07  $\text{min}^{-1}$  in multiple sclerosis,<sup>8,15</sup> to 0.01–1.5  $\text{min}^{-1}$  in tumours.<sup>6</sup> A leakage space  $v_l$  has been measured<sup>8</sup>; this is the fraction of the lesion volume that is accessible to the leaking Gd-DTPA tracer. We consider two kinds of lesion:

first, "partly water" lesions (e.g., multiple sclerosis, tumours) where  $v_l < 1$  (e.g., in MS  $v_l = 0.18-0.49^{15}$ ); it probably corresponds to the extracellular space and in general its size is unknown. Second, "completely water" lesions  $v_l = 1$  (e.g., in the retina, where all of the vitreous humour is accessible to tracer). Since the value of  $v_l$  is known a priori in completely water lesions, this can be used to simplify the theoretical model used to estimate permeability. The Simplified Early Enhancement (SEE) method<sup>16</sup> uses this prior knowledge to estimate permeability in the retina using simple computation.

Other workers have studied the dynamics of the uptake of Gd-DTPA without explicitly calculating permeability values. Some have chosen to use a bolus injection,<sup>6</sup> whilst others have used a constant infusion-rate injection.<sup>17,18</sup> There is clearly some uncertainty in the literature regarding the relative merits of bolus and infusion injections, and in this paper we compare the relative advantages of the two methods for measuring permeability. We concentrate on the lower values of  $k$ , in the range  $10^{-4}-10^{-1} \text{ min}^{-1}$ , since this is where the time to reach an acceptable enhancement may be long ( $>10 \text{ min}$ ), and an infusion injection might be thought worthwhile. At high values of  $k$  ( $>0.1 \text{ min}^{-1}$ ), the time to peak enhancement is short ( $<10 \text{ min}$ ), and an infusion injection would not be considered, because it would have such a short duration as to be not significantly different from a bolus.

For the constant infusion rate method, we derive expressions for the plasma and tissue concentration of tracer as a function of time. We extend the SEE method to estimate permeability in retinal lesions from infusion data, and we demonstrate its application to published data. Using computer simulations, we investigate whether a constant plasma concentration can be obtained with an infusion injection, and we compare the two methods of injecting (bolus and infusion), according to the following criteria: 1) the tissue concentration that can be achieved in a given time after the start of injection; 2) the imaging time required to achieve an acceptable enhancement; 3) the total amount of tracer that has to be injected; 4) how the accuracy of the permeability estimate is maintained in the presence of a reduction in renal function; and 5) how much error arises from the simplifying assumptions made in the SEE method for estimating retinal permeability.

## THEORY

### Bolus Injection

After intravenous (IV) injection of a bolus dose  $D^{\text{bol}}$  mmol/kg body weight, given at time  $t = 0$ , the plasma concentration decays biexponentially<sup>8</sup>

$$C_p^{\text{bol}}(t) = D^{\text{bol}} \sum_{i=1}^2 a_i e^{-m_i t} \quad (1)$$

where  $i = 1$  describes the early mixing phase between plasma and extracellular water, and  $i = 2$  describes the later renal excretion phase. In humans, the data of Weinmann et al.<sup>19</sup> fit<sup>8</sup>  $a_1 = 3.99 \text{ kg/liter}$ ,  $a_2 = 4.78 \text{ kg/liter}$ ,  $m_1 = 0.144 \text{ min}^{-1}$ ,  $m_2 = 0.0111 \text{ min}^{-1}$ . In rabbits<sup>14</sup>  $a_1 = 4.37 \text{ kg/liter}$ ,  $a_2 = 2.59 \text{ kg/liter}$ ,  $m_1 = 0.24 \text{ min}^{-1}$ ,  $m_2 = 0.0094 \text{ min}^{-1}$ . The resulting tissue concentration is<sup>8</sup>

$$C_t^{\text{bol}}(t) = D^{\text{bol}} k \sum_{i=1}^2 a_i (e^{-m_3 t} - e^{-m_i t}) / (m_i - m_3) \quad (2)$$

where  $m_3 = k/v_l$ . In retinal lesions the permeability is small<sup>14</sup> ( $k \approx 10^{-3} \text{ min}^{-1}$ ), the lesion is completely water ( $v_l = 1$ ), and  $m_i \geq 10^{-2}$  (see above), so  $k \ll m_i$ . This implies that at realistic times ( $t < 100 \text{ min}$ )  $kt \ll 1$ , so Eq. (2) can be simplified to

$$C_t^{\text{bol}}(t) = D^{\text{bol}} k \sum_{i=1}^2 a_i (1 - e^{-m_i t}) / m_i \quad (k \ll m_i, kt \ll 1) \quad (3)$$

Thus, at short times ( $t \ll m_i^{-1}$ ) the tissue concentration in retinal lesions increases linearly with time:

$$C_t^{\text{bol}}(t) = D^{\text{bol}} kt \sum_{i=1}^2 a_i \quad (k \ll m_i, t \ll m_i^{-1}) \quad (4)$$

Note that the two strong conditions in Eq. (4) imply the weaker condition  $kt \ll 1$  in Eq. (3).

### Constant Infusion Rate Injection

Let the IV infusion rate be  $\dot{D}^{\text{inf}}$  mmol/kg  $\text{min}^{-1}$ , starting at time  $t = 0$ . This injection can be treated as a series of small doses (doselets)  $\Delta D = \dot{D}^{\text{inf}} \Delta t'$ , each lasting time  $\Delta t'$ . The plasma concentration resulting from a doselet given at time  $t'$  is then, from Eq. (1),

$$\Delta C_p(t) = \dot{D}^{\text{inf}} \Delta t' \sum_{i=1}^2 a_i e^{-m_i(t-t')} \quad (5)$$

and the total plasma concentration is the sum of the contributions from each doselet:

$$\begin{aligned} C_p^{\text{inf}}(t) &= \lim_{\Delta t' \rightarrow 0} \sum_{t'=0}^t \Delta C_p(t) \\ &= \dot{D}^{\text{inf}} \sum_{i=1}^2 a_i (1 - e^{-m_i t}) / m_i \end{aligned} \quad (6)$$

Shortly after the start of infusion, the plasma concentration increases linearly with time:

$$C_p^{\text{inf}}(t) = \dot{D}^{\text{inf}} t \sum_{i=1}^2 a_i \quad (m_i t \ll 1) \quad (7)$$

and at long times the plasma concentration becomes constant:

$$C_p^{\text{inf}}(t) = \dot{D}^{\text{inf}} \sum_{i=1}^2 a_i / m_i \quad (m_i t \gg 1) \quad (8)$$

Similarly, using Eq. (2), the tissue concentration at any time is the sum of the contributions from each doselet:

$$C_t^{\text{inf}}(t) = \dot{D}^{\text{inf}} k \sum_{i=1}^2 \frac{a_i}{m_i - m_3} \times \left( \frac{1 - e^{-m_3 t}}{m_3} - \frac{1 - e^{-m_i t}}{m_i} \right) \quad (9)$$

In retinal lesions we can make the same approximations as for Eq. (3) and then:

$$C_t^{\text{inf}}(t) = \dot{D}^{\text{inf}} k \sum_{i=1}^2 a_i (m_i t + e^{-m_i t} - 1) / m_i^2 \quad (k \ll m_i, kt \ll 1) \quad (10)$$

Thus, at short times the tissue concentration increases *quadratically* with time:

$$C_t^{\text{inf}}(t) = \dot{D}^{\text{inf}} k t^2 \sum_{i=1}^2 a_i / 2 \quad (k \ll m_i, t \ll m_i^{-1}) \quad (11)$$

At longer times, the concentration increases *linearly* with time:

$$C_t^{\text{inf}}(t) = \dot{D}^{\text{inf}} k t \sum_{i=1}^2 a_i / m_i \quad (m_i^{-1} \ll t \ll k^{-1}) \quad (12)$$

### Hybrid Injection

The constant infusion rate injection does not provide a constant plasma concentration until a time at least  $\sim 1/m_i$  after the start of injection [Eq. (8)]. This must be satisfied for both components,  $i = 1$  and  $2$ . For the long ( $i = 2$ ) component, this is  $\sim 100$  min, which is unacceptably long. By using a hybrid injection, consisting of bolus and constant infusion injections in the correct proportion, a constant plasma curve can be reached much more quickly. From Eqs. (1) and (6), the plasma concentration after a hybrid injection is

$$C_p^{\text{hyb}}(t) = \sum_{i=1}^2 a_i [(D^{\text{bol}} - \dot{D}^{\text{inf}} / m_i) e^{-m_i t} + \dot{D}^{\text{inf}} / m_i] \quad (13)$$

and the amplitude of the slow exponential ( $i = 2$ ) can be nulled by choosing an infusion rate of

$$\dot{D}^{\text{inf}} = m_2 D^{\text{bol}} \quad (14)$$

### Dose Efficiency

We compare the tissue concentration achieved by a bolus with that achieved by an infusion of the same amount of tracer over the same time. Suppose the enhancement is observed from time  $t = 0$  to time  $t = t_{\text{inf}}$ . Then the amount of tracer used under the infusion procedure is  $\dot{D}^{\text{inf}} t_{\text{inf}}$ , and we compare this to a bolus  $D^{\text{bol}} = \dot{D}^{\text{inf}} t_{\text{inf}}$ . The ratio of tissue concentrations at  $t_{\text{inf}}$  for a bolus and an infusion, in the case of a retinal lesion [Eqs. (3) and (10)], is

$$R^{\text{bol/inf}} = \frac{C^{\text{bol}}(t_{\text{inf}})}{C^{\text{inf}}(t_{\text{inf}})} = \frac{\sum_{i=1}^2 a_i (1 - e^{-m_i t_{\text{inf}}}) t_{\text{inf}} / m_i}{\sum_{i=1}^2 a_i (m_i t_{\text{inf}} + e^{-m_i t_{\text{inf}}} - 1) / m_i^2} \quad (k \ll m_i, kt_{\text{inf}} \ll 1) \quad (15)$$

and depends on time but not on the permeability. This is valid for  $k \ll m_i \approx 0.01 \text{ min}^{-1}$ . At short times, the bolus is twice as effective as the infusion:

$$R^{\text{bol/inf}} \rightarrow 2 \quad (t_{\text{inf}} \ll m_i^{-1} \ll k^{-1}) \quad (16)$$

and at longer times they are equally effective:

$$R^{\text{bol/inf}} \rightarrow 1 \quad (m_i^{-1} \ll t_{\text{inf}} \ll k^{-1}) \quad (17)$$

Thus, in retinal lesions the bolus is always more effective than the constant infusion injection in reaching a particular required concentration.

### Reduction in Renal Function

The accuracy of the permeability estimate relies on the plasma concentration being known [Eqs. (1) and (6)]. We have assumed normal values; however, a potential source of inaccuracy is a reduction in renal function, through kidney malfunction, as this will alter the clearance of tracer from the plasma. The plasma curve

will then not be that predicted by inserting normal values of the plasma parameters  $a_1$ ,  $a_2$ ,  $m_1$ , and  $m_2$  into Eq. (1) or (6). Ideally, the estimate of permeability should be robust with respect to variation in the plasma parameters. All four of the parameters depend on the size of the plasma and extracellular spaces.<sup>8</sup> In addition,  $m_1$  is proportional to the permeability from capillary to extracellular space in the whole body, and  $m_2$  is proportional to the glomerular filtration rate. We therefore expect the main effect of a reduction in renal function to be a reduction in  $m_2$ . The error in estimating plasma concentration will increase with time (at short times  $C_p$  is independent of  $m_2$ ). We therefore expect the resulting fractional error in permeability to increase with time for both methods, but to be independent of dose and permeability.

#### *Simplified Early Enhancement Method for Estimating Permeability – Extension to Infusion Injection*

In this section, we extend the Simplified Early Enhancement (SEE) method for estimating retinal permeability, previously only derived for a bolus injection,<sup>8</sup> to the case of an infusion injection. The estimation of permeability  $k$  from the enhancement  $E$  can be separated into two processes. First, the tissue concentration is estimated from enhancement. We define enhancement to be the increase in signal after injection of the tracer, divided by the signal preinjection. For a spin-echo this is<sup>16</sup>

$$E = e^{-R_2 C_t TE} \times \frac{1 - 2e^{-(TR-TE/2)(T_{10}^{-1} + R_1 C_t)} + e^{-TR(T_{10}^{-1} + R_1 C_t)}}{1 - 2e^{-(TR-TE/2)T_{10}^{-1}} + e^{-TR T_{10}^{-1}}} - 1 \quad (18)$$

where  $T_{10}$  is the  $T_1$  before injection, and  $R_1$ ,  $R_2$  are the  $T_1$  and  $T_2$  relaxivities. A linear approximation to this is<sup>16</sup>:

$$E = R_1 T_k C_t \quad (R_1 C_t \ll TR^{-1}) \quad (19)$$

where

$$T_k = \frac{TR e^{-TR/T_{10}}}{1 - e^{-TR/T_{10}}} \quad (TE \ll T_2, TR) \quad (20)$$

and  $C_t$  can be estimated from  $E$  using these two equations. The linear approximation breaks down at higher values of tissue concentration (and hence enhancement), in which case Eq. (18) can be inverted exactly, for example by an iterative procedure.<sup>16</sup>

Second, permeability is estimated from tissue concentration. The equations for tissue concentration in a retinal lesion [Eqs. (3) and (10)] can be rearranged to give permeability for a bolus injection

$$k = \frac{C_t^{\text{bol}}(t)}{D^{\text{bol}} \sum_{i=1}^2 a_i (1 - e^{-m_i t}) / m_i} \quad (k \ll m_i, t \ll k^{-1}) \quad (21)$$

and for an infusion injection

$$k = \frac{C_t^{\text{inf}}(t)}{\dot{D}^{\text{inf}} \sum_{i=1}^2 a_i (m_i t + e^{-m_i t} - 1) / m_i^2} \quad (k \ll m_i, t \ll k^{-1}) \quad (22)$$

Eq. (21), used in conjunction with Eq. (19) to obtain  $C_t$  from  $E$ , is the Simplified Early Enhancement method given by Tofts and Berkowitz<sup>16</sup>; Eq. (22) represents its extension to a constant infusion rate injection. Notice that the denominators are the integral of the plasma concentration [see Eqs. (1) and (6)], and that these equations can also be obtained by ignoring back-flow and writing  $C_t(t) = k \int C_p(t) dt$ . These equations both assume the permeability is small (i.e.  $k \ll m_i$  and  $kt \ll 1$ ). We expect that the fractional error in  $k$  arising from this assumption will increase with time and permeability, and be independent of dose. The size of the error is given below (see Results). If the error is unacceptably high, exact iterative solutions to Eqs. (2) and (9) can be used, in place of Eqs. (21) and (22), to obtain  $k$  from  $C_t$ .<sup>16</sup>

## RESULTS

### *Constancy of Plasma Concentration*

The time course of the plasma concentration and the tissue concentrations for bolus, constant infusion, and hybrid injections, predicted by the above theory, are shown in Fig. 1 for a range of permeabilities. The plasma concentration after a bolus injection decays bi-exponentially [Eq. (1)], whilst after the infusion [Eq. (6)] it rises approximately linearly [as predicted by Eq. (7)] towards a plateau [Eq. (8)]. The bolus and infusion methods are both unsuccessful in achieving a constant plasma concentration in a reasonable time; however, the hybrid injection [Eqs. (13) and (14)] is effective, as can be seen in the figure.

The tissue concentration for a low permeability ( $k = 0.001 \text{ min}^{-1}$ ), completely water lesion ( $v_t = 1$ ) is

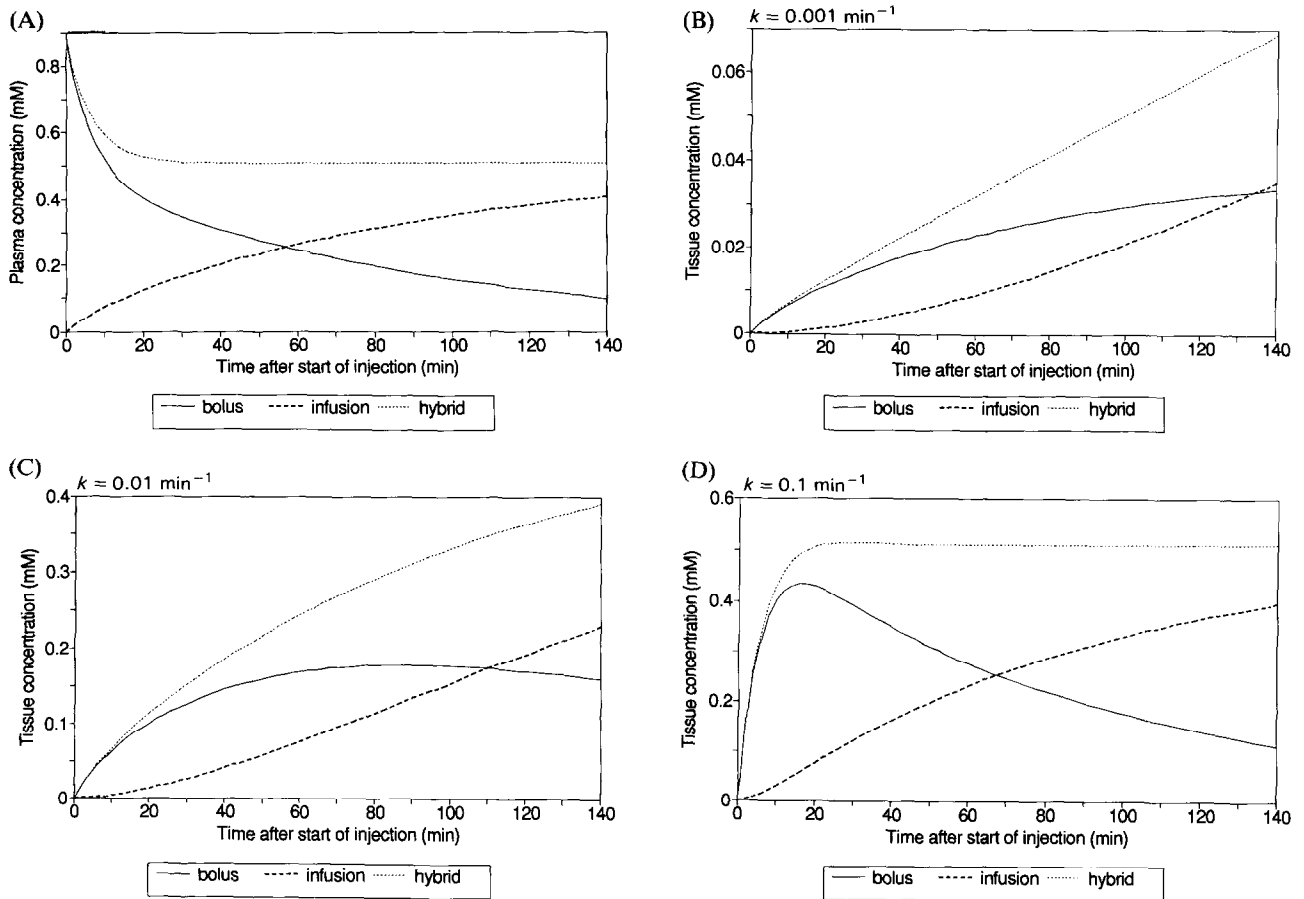


Fig. 1. Time course of plasma and tissue concentrations in a human after a bolus injection ( $D^{\text{bol}} = 0.1 \text{ mmol/kg}$ ), a constant infusion rate injection ( $\dot{D}^{\text{inf}} = 0.00111 \text{ mmol/kg min}^{-1}$ ) and a hybrid injection consisting of the bolus followed by the infusion. Plasma constants are  $a_1 = 3.99 \text{ kg/liter}$ ,  $a_2 = 4.78 \text{ kg/liter}$ ,  $m_1 = 0.144 \text{ min}^{-1}$ ,  $m_2 = 0.0111 \text{ min}^{-1}$ .<sup>8</sup> (A) Plasma; 20 min after the start of the hybrid injection the plasma concentration is constant. (B) Tissue (low permeability  $k = 0.001 \text{ min}^{-1}$ ). Twenty minutes after the start of the hybrid injection, the tissue concentration is rising linearly with time. (C) Tissue (medium permeability  $k = 0.01 \text{ min}^{-1}$ ). (D) Tissue (high permeability  $k = 0.1 \text{ min}^{-1}$ ). Twenty minutes after the start of the hybrid injection, the tissue concentration is constant.

shown in Fig. 1B. At short times it increases linearly with time for the bolus [Eq. (4)], and quadratically with time for the infusion [Eq. (11)]. At longer times the linear rise is seen for the infusion [Eq. (12)]. In contrast, the tissue concentration after the hybrid injection rises linearly over the whole period of time. At medium and high permeabilities ( $k = 0.01 \text{ min}^{-1}$ , Fig. 1C;  $k = 0.1 \text{ min}^{-1}$ , Fig. 1D) the tissue concentration rises in a nonlinear way for all injection types. For the high permeability lesion ( $k = 0.1 \text{ min}^{-1}$ ), after a hybrid injection the tissue concentration soon reaches the plasma concentration, and then remains constant. Curves for partly water lesions show similar features (data not shown). The accuracy of the hybrid injection will depend on how accurately the value of  $m_2$  is known [Eq. (14)];

however, if a constant plasma concentration is required, then a hybrid injection is a more effective way to achieve it than is an infusion.

#### Tissue Concentration Achieved

In order to compare tissue concentrations from the two injection types, we suppose that a particular dose  $D^{\text{bol}}$  can be given either as a bolus at time  $t = 0$  or as an infusion, starting at time  $t = 0$ , of duration  $t_{\text{inf}}$  and dose rate  $\dot{D}^{\text{inf}} = D^{\text{bol}}/t_{\text{inf}}$ . We compare the tissue concentrations achieved [Eqs. (2) and (9)] a time  $t_{\text{inf}}$  after the start of each injection type. Figure 2 shows the tissue concentrations after a dose of  $0.1 \text{ mmol/kg}$  for a completely water lesion with a range of permeabilities. The ratio of these concentrations (bolus:infusion)

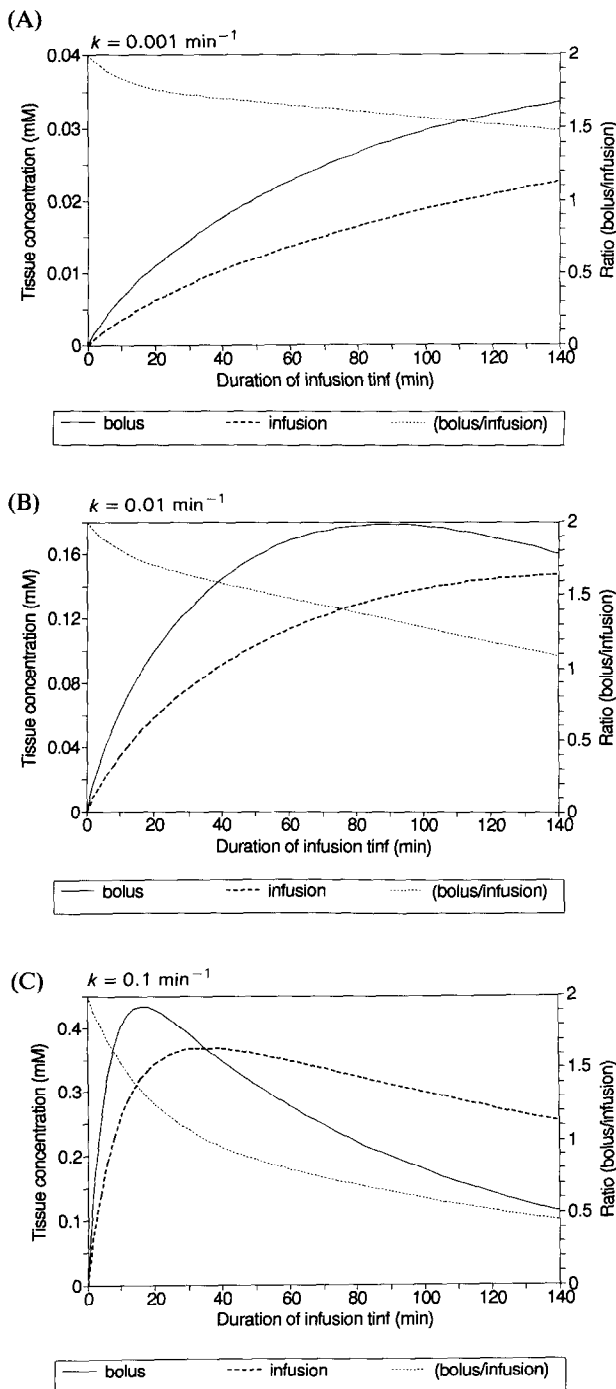


Fig. 2. Comparison of the effect of delivering the same total amount of Gd-DTPA tracer by a bolus injection (at time  $t = 0$ ) and by a constant infusion-rate injection starting at time  $t = 0$  and of duration  $t_{inf}$ . Graphs of the tissue concentration at time  $t_{inf}$  after the bolus and at the end of the infusion are shown. The ratio of tissue concentration from a bolus to tissue concentration from an infusion injection (right hand axis) is always  $> 1$  for realistic times.  $D^{bol} = 0.1 \text{ mmol/kg}$ ;  $\dot{D}^{inf} = D^{bol}/t_{inf}$ . Plasma constants as in Fig 1. (A) Permeability  $k = 0.001 \text{ min}^{-1}$ . (B)  $k = 0.01 \text{ min}^{-1}$ . (C)  $k = 0.1 \text{ min}^{-1}$ .

[Eq. (15)] is also shown. At low permeability ( $k = 0.001 \text{ min}^{-1}$ ; Fig. 2A) the ratio is 2 for short infusions, as predicted by Eq. (16). For infusions of duration up to 1 h, a realistic upper limit, the bolus achieves a higher concentration at the low and medium permeabilities (at  $t_{inf} = 60 \text{ min}$ , the ratio is 1.7 for  $k = 0.001 \text{ min}^{-1}$  and 1.5 for  $k = 0.01 \text{ min}^{-1}$ ). The higher permeability lesion ( $k = 0.1 \text{ min}^{-1}$ ; Fig. 2C) reaches its highest tissue concentration 16 min after a bolus injection. A 16 min infusion of the same amount of tracer produces a tissue concentration about 1.3 times lower; and infusions of any length produce lower tissue concentrations than that achieved 16 min after a bolus. The decline in the ratio of concentrations (bolus/infusion) seen in Fig. 2C to less than 1 at longer times is consistent with Eq. (17), since the condition for low permeability ( $k \ll m_i$ ) is not satisfied for the high permeability lesion. Curves for partly water lesions with the same range of permeabilities show similar features (data not shown).

#### Imaging Time Required

The total imaging time required is generally determined by having to wait for a tissue concentration, and hence an enhancement  $E$ , to build up that is sufficiently large that it can be measured precisely. The random error in the estimate of permeability  $\sigma_k/k \approx \sqrt{2}/(E \text{ SNR}_0)$ , where  $\text{SNR}_0$  is the signal-to-noise ratio in the preinjection image.<sup>16</sup> Ideal values for enhancement are  $E \approx 1-3$  for retinal lesions and  $E \approx 0.5$  for MS lesions and tumours, since above this nonlinearity of signal enhancement with tissue concentration becomes important [this was shown by simulations using Eqs. (18)–(20)]. Figure 2 shows that for a variety of permeabilities and a given amount of tracer, up to a time 140 min, any particular tissue concentration is always achieved faster if the tracer is given as a bolus than if it is given as the equivalent infusion.

The imaging time should not be allowed to become so long that variations in renal function affect the plasma curve significantly. We show below that this could produce an error of 10% at 40 min after injection of a bolus. If an imaging time longer than about 40 min would be required to achieve an acceptable enhancement, then ideally the investigation should be redesigned to use a larger dose, so that an acceptable enhancement is achieved earlier.

#### Total Amount of Tracer Required

If we require to reach a particular tissue concentration in a given scanning time, then the ratio of required infusion dose to required bolus dose is equal to the ratio of tissue concentrations for the same bolus and infusion dose. This follows from the fact that tissue

concentration is proportional to dose. This ratio is shown in Fig. 2, and is typically 1.3–1.7 at realistic times (up to 1 h), as stated above. Thus the bolus requires less total dose of tracer than does the infusion to achieve a useful enhancement in a given time.

#### Accuracy in the Presence of Reduced Renal Function

The magnitude of the error produced by assuming normal renal function when it was in fact reduced to 50% of its normal value is shown in Fig. 3 (upper 2 lines). A normal value of  $m_2$  was used to calculate the tissue concentration [Eqs. (2) and (9)], and also to estimate permeability from this by the SEE method [Eqs. (21) and (22)]. A reduced value of  $m_2$  (50% of the normal value) was then used to calculate a second value of tissue concentration, from which permeability was again estimated using the normal value. The difference in these two estimates is caused solely by the reduction in actual  $m_2$  (i.e., GFR or renal function), regardless of any other errors caused by the approximations inherent in the SEE method. Other methods of estimating permeability would show similar dependence on altered renal function since all methods are sensitive to alterations in  $\int C_p(t) dt$  [the denominator of Eqs. (21) and (22)]. As expected, the error increases with time, is independent of dose, and is approximately

independent of permeability over the range  $k = 0\text{--}0.01 \text{ min}^{-1}$ .

#### Accuracy of the Simplified Early Enhancement Method

The SEE method [Eqs. (21) and (22)] assumes that the permeability is small. Simulation shows that the error increases approximately linearly with time and with permeability (we expect it to be proportional to  $kt$ ). At any particular time it is approximately 60% higher for the bolus injection (since the bolus was given earlier than most of the infusion tracer) and is independent of dose. An example is given in Fig. 3 (upper 2 lines), for  $k = 0.001 \text{ min}^{-1}$ .

#### Relative Accuracy of Bolus and Infusion Injections

The errors at a particular time (shown in Fig. 3) are higher for the bolus than for the infusion, and at first sight this suggests the infusion is preferable. For example, 50 min after a bolus injection, the error arising from the SEE assumption that permeability is small is 2.9%, whereas 50 min after the start of an infusion it is only 1.8% ( $k = 0.001 \text{ min}^{-1}$  in Table 1). However, we know from Fig. 2 that a particular tissue concentration, and hence enhancement, is reached earlier with a bolus than with an infusion of the same amount of tracer. A bolus therefore allows permeability to be measured earlier than does an infusion (for a given total amount of tracer). Continuing the above example, after a 50-min infusion of  $0.002 \text{ mmol/kg min}^{-1}$  (total dose  $0.1 \text{ mmol/kg}$ ), the tissue concentration is  $0.012 \text{ mM}$ ; a bolus of  $0.1 \text{ mmol/kg}$  reaches this tissue concentration at the earlier time of 23 min, when the error from the SEE assumption of small permeability is only 1.3% (i.e., less than that of the 50-min infusion). Similarly the error arising from reduced renal function, for a particular tissue concentration, is also lower for the bolus. Similar conclusions also apply for the medium permeability ( $k = 0.01 \text{ min}^{-1}$ ; see Table 1). At high permeability ( $k = 0.1 \text{ min}^{-1}$ ), the errors arising from reduced renal function are lower for the bolus. The SEE method is not applicable because the condition  $k \ll m_2$  [Eqs. (21) and (22)] is not met; and a more accurate alternative is the Early Enhancement method.<sup>16</sup> We have not evaluated this for an infusion injection, since the infusion becomes increasingly unattractive at high permeabilities, as the time to peak enhancement decreases, as seen in Fig. 2C.

For the low and medium permeabilities, it is more valid to compare errors, for both injection methods, at the same tissue concentration, not at the same time (for the same total dose), and this is done in Fig. 4 for  $k = 0.001 \text{ min}^{-1}$ . For any particular tissue concentra-

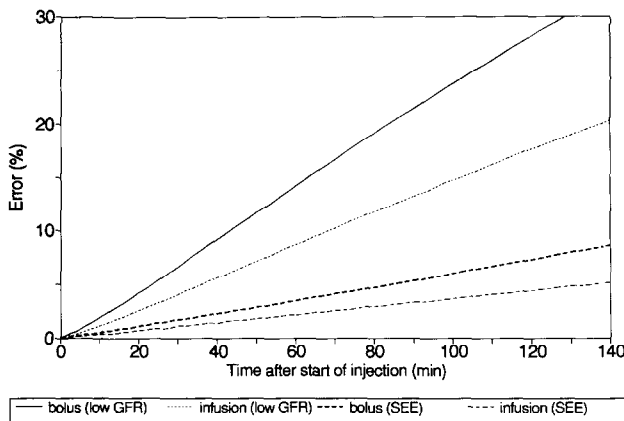


Fig. 3. Time dependence of errors in estimating permeability  $k$  from the tissue concentration. Curves are shown for the bolus and infusion injections,  $k = 0.001 \text{ min}^{-1}$ , for two sources of error: (1) the effect of using the Simplified Early Enhancement method assumption that permeability is small (keeping renal function normal) (SEE; lower 2 lines) and (2) the additional effect of an unexpected 50% reduction in renal function (low GFR; upper 2 lines). The effects are independent of dose. At lower permeability ( $k = 0.0001 \text{ min}^{-1}$ ), the error of the SEE method is  $< 1\%$ , and the error from reduced renal function is unchanged.

Table 1. Example of errors and imaging times required for bolus and infusion injections

	Time after start of injection (min)	Type of injection	SEE error (%)	GFR error (%)	Tissue concentration (mM)
Low permeability ( $k = 0.001 \text{ min}^{-1}$ )	50	Bolus 0.1 mmol/kg	2.9	11.8	0.021
	50	Infusion 0.002 mmol/kg $\text{min}^{-1}$ (total 0.1 mmol/kg)	1.8	7.2	0.012
	23	Bolus 0.1 mmol/kg	1.3	5.0	0.012
Medium permeability ( $k = 0.01 \text{ min}^{-1}$ )	50	Bolus 0.1 mmol/kg	25	10	0.16
	50	Infusion 0.002 mmol/kg $\text{min}^{-1}$ (total 0.1 mmol/kg)	16	6	0.10
	21	Bolus 0.1 mmol/kg	11	4	0.10

tion, the bolus has less error arising from reduced renal function (low GFR) than does the infusion, and it provides a more accurate estimate of  $k$  using the SEE method. The time to achieve a particular tissue concentration is also shown, and is lower for a bolus (as also deduced above from Fig. 2).

#### Measurement of Permeability From Constant Infusion Rate Data

Wu et al.<sup>18</sup> have published enhancement curves for several retinal lesions in rabbits after constant infusion rate injections. Using our exact model [Eqs. (9)

and (18)], the rabbit plasma parameters of Berkowitz et al.<sup>14</sup> and measured relaxivities<sup>20</sup> we are able to fit their data. We used a  $T_{10}$  value for the vitreous humor of 4 s.<sup>14</sup> Because their data do not pass through the origin as they should (in fact they report  $E = 0.36$  at  $t = 0$ ), we made a small correction by subtracting 0.36 from all the  $E$  values. Figure 5 shows data from a rabbit vitreous 2 days after retinal cryotherapy (their animal #19419). The quadratic rise in enhancement at early times [predicted by our Eq. (11)] can be clearly seen. Our exact model with  $k = 2.78 \times 10^{-3} \text{ min}^{-1}$  produced a curve that fits their corrected data. At later times the rise of enhancement with time is linear up to high values ( $>5$ ), even though the rise of tissue concentration rise is not linear (see Fig. 5). This is because the quadratic rise in tissue concentration is offset by the less-than-linear rise of enhancement with concentration.

The SEE method can be used to estimate an approximate value of permeability from a single enhancement value at a particular time. Using the corrected value of  $E = 1.81$  at time  $t = 30 \text{ min}$ , we obtain  $k = 2.94 \times 10^{-3} \text{ min}^{-1}$ , in good agreement with the fitted value ( $2.78 \times 10^{-3} \text{ min}^{-1}$ ). Modelling of the data taken 2 days after laser photocoagulation (animal #19420) showed similar effects, and gave  $k = 1.11 \times 10^{-3} \text{ min}^{-1}$ .

The  $PS$  product for a lesion where the leakage is contained within the slice thickness  $SLT$  is<sup>14,16</sup>

$$PS = kA_{ROI}SLT \quad (23)$$

where  $A_{ROI}$  is the area of the region of interest used to measure the enhancement (this must be large enough to contain all the enhancing vitreous). This product is independent of the particular slice thickness and region used, and is a true physiological measurement of permeability. Using the data of Wu et al.<sup>18</sup> ( $A_{ROI} = 20 \text{ mm}^2$ ,  $SLT = 2 \text{ mm}$ ), we estimate that for the cryo-

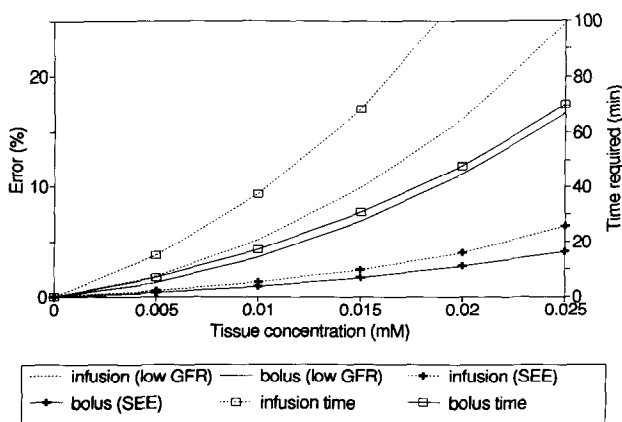


Fig. 4. Magnitude of error in estimating permeability  $k$  from tissue concentration, as a function of tissue concentration, given the same total amount of tracer used by the time the enhancement is measured. Curves are shown for the bolus and infusion injections, with  $k = 0.001 \text{ min}^{-1}$ . Curves are: (1) the error arising from using the Simplified Early Enhancement (SEE) assumption that permeability is small; (2) the error arising from reduced renal function (low GFR); and (3) the time to reach the specified tissue concentration (right hand axis).

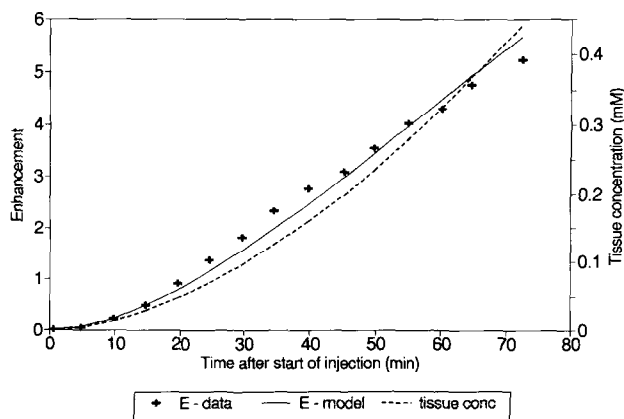


Fig. 5. Enhancement data (E-data) from Wu et al.<sup>18</sup> ( $\dot{D}^{\text{inf}} = 0.015 \text{ mmol/kg min}^{-1}$ ) using a SE300/12 sequence fit our model (E-model) using  $T_{10} = 4 \text{ s}$ ;  $R_1 = 4.5 \text{ s}^{-1} \text{ mM}^{-1}$ ,  $R_2 = 5.5 \text{ s}^{-1} \text{ mM}^{-1}$  (measured at 1.5 T, 21°C; see Ref. 20) and give  $k = 2.78 \times 10^{-3} \text{ min}^{-1}$ ,  $PS = 1.11 \times 10^{-3} \text{ cm}^{-2} \text{ min}^{-1}$ . The model shows that the tissue concentration (tissue conc) rises nonlinearly with time. The data have been corrected by subtraction of a constant offset of 0.36 to make them pass through the origin.

therapy lesion  $PS = 1.1 \times 10^{-4} \text{ cm}^3 \text{ min}^{-1}$ , and for the photocoagulation lesion  $PS = 0.44 \times 10^{-4} \text{ cm}^3 \text{ min}^{-1}$ .

## DISCUSSION

The quadratic rise in enhancement seen at short times in the infusion data of Wu et al.<sup>18</sup> (Fig. 5) support our model. The close agreement of the SEE estimate with the exact model supports the use of SEE, which is convenient to compute and requires only a single measurement of enhancement. We have used Wu et al.'s data to demonstrate our exact model and the SEE method; however, the estimates may be inaccurate for two reasons. Firstly, the enhancement in parts of the region of interest may be large enough to leave the linear part of the enhancement vs. tissue concentration curve. Our simulations, using Eqs. (18)–(20), show that for retinal lesions ( $T_{10} = 4 \text{ s}$ ), a SE300/10 sequence, as used by Wu et al.<sup>18</sup> gives a 10% nonlinearity at an enhancement  $E = 2.3$ . Even though the exact relationship between concentration and enhancement is known for a homogenous region of tissue [Eq. (18)], it is not possible to estimate the relationship for a heterogeneous region of tissue, unless the distribution of enhancement values within the region is known. Ideally, the peak enhancement within the region should not exceed about 2. Secondly because the capillaries may be occluded by the laser, the functional form of

the Gd-DTPA plasma curve may differ from the arterial form,<sup>21</sup> and erroneously low values of permeability may be estimated.

Although modelling of the distribution of labelled DTPA has been undertaken previously,<sup>22–25</sup> our work represents several important advances in the application of tracer methodology to MRI. This is the first time that a constant infusion rate injection has been explicitly considered, and that it has been compared to a bolus according to the criteria of this paper. Fenstermacher<sup>22</sup> states in his review that “the bolus injection method of administration is simple and almost always generates usable experimental results, whereas the constant plasma activity approach employs fairly complex infusion schedules, which often fail to produce reasonably steady plasma concentrations and acceptable data.” Blasberg et al.<sup>24,25</sup> concluded that “bolus intravenous administration of the test-solute yields the optimal plasma concentration–time relationship,” although no detailed analysis was given. Thus, our findings are consistent with previous work. The emphasis of the earlier work<sup>22–25</sup> was on radioactively labelled tracers, including DTPA, injected into animal models, where plasma concentrations can be monitored as a function of time to determine  $\int C_p dt$ . In this paper we have focused on Gd-labelled DTPA injected into human subjects and monitored by MRI. Direct monitoring of plasma concentration is then invasive and inconvenient, and we have used analytic expressions for the plasma concentration. A noninvasive method for monitoring the plasma concentration has been published,<sup>26</sup> but this requires MRI examination of the aorta, which cannot usually be carried out simultaneously with imaging of the brain or retina. The earlier work used more elaborate models, including four exponential terms for the plasma concentration.<sup>25</sup> We have found a simple model, with two exponential terms for the plasma, fits the data.<sup>8</sup>

We have demonstrated that the bolus injection of Gd-DTPA is a more efficient and a more accurate procedure than a constant-rate infusion, providing a result with less total tracer or with less imaging time. Although the hybrid injection achieves a constant plasma concentration most quickly, variations with time of the plasma concentration can be taken into account in the calculation of permeability by the SEE method [Eqs. (21) and (22)], and therefore constancy of plasma concentration need no longer be a criterion by which to judge an injection procedure. The bolus is more practical, because no special equipment is needed, the only requirement being that the time of injection is accurately noted. It may also allow the measurement of blood volume, by tracking the bolus with a gradient-echo

for the first 30 s after injection.<sup>6,27</sup> This is a "free" measurement, requiring no extra tracer or scanner time. Although we have used human plasma parameters in our simulations, those in experimental animals are not substantially different, and our conclusions apply as much to investigations into experimental lesions as they do to clinical measurements on human subjects.

## REFERENCES

- Gadian, D.G.; Payne, J.A.; Bryant, D.J.; Young, I.R.; Carr, D.H.; Bydder, G.M. Gadolinium-DTPA as a contrast agent in MR imaging: Theoretical projections and practical observations. *J. Comput. Assist. Tomogr.* 9: 242-251; 1985.
- Sze, G. New applications of MR contrast agents in neuroradiology. *Neuroradiology* 32:421-438; 1990.
- Wilson, C.A.; Fleckenstein, J.L.; Berkowitz, B.A.; and Green, M.E. Proliferative diabetic retinopathy: Evaluation using contrast-enhanced magnetic resonance imaging. *J. Diab. Comp.* 6:223-229; 1992.
- Grossman, R.I.; Gonzales-Scarano, F.; Atlas, S.W.; Galetta, S.; Silberberg, D.H. Multiple sclerosis: Gadolinium enhancement in MR imaging. *Radiology* 161:721-725; 1986.
- Miller, D.H.; Rudge, P.; Johnson, G.; Kendall, B.E.; MacManus, D.G.; Moseley, I.F.; Barnes, D.; McDonald, W.I. Serial gadolinium enhanced magnetic resonance imaging in multiple sclerosis. *Brain* 111:927-939; 1988.
- Gowland, P.; Mansfield, P.; Bullock, P.; Stehling, M.; Worthington, B.; Firth, J. Dynamic studies of gadolinium uptake in brain tumours using inversion-recovery echo-planar imaging. *Magn. Reson. Med.* 26:241-258; 1992.
- Bradbury, M. *The Concept of a Blood-Brain Barrier*. New York: Wiley; 1979.
- Tofts, P.S.; Kermode, A.G. Measurement of the blood-brain barrier permeability and leakage space using dynamic MR imaging. 1. Fundamental concepts. *Magn. Reson. Med.* 17:357-367; 1991.
- Tofts, P.S.; Kermode, A.G. Measurement of blood-brain barrier permeability using Gd-DTPA scanning. *Magn. Reson. Imaging* 7(Suppl 1):150; 1989.
- Tofts, P.S.; Kermode, A.G.; Barker, G. Measurement of the blood-brain barrier permeability using dynamic Gd-DTPA scanning. In: Book of abstracts: Eighth Annual Meeting of the Society of Magnetic Resonance in Medicine, Vol. 2. Berkeley, CA:SMRM; 1989:805.
- Larsson, H.B.W.; Stubgaard, M.; Frederiksen, J.L.; Jensen, M.; Henriksen, O.; Paulson, O.B. Quantitation of blood-brain barrier defect using MRI and Gadolinium-DTPA in acute multiple sclerosis. In: Book of abstracts: Eighth Annual Meeting of the Society of Magnetic Resonance in Medicine, Vol. 2. Berkeley, CA:SMRM; 1989:744.
- Larsson, H.B.W.; Stubgaard, M.; Frederiksen, J.L.; Jensen, M.; Henriksen, O.; Paulson, O.B. Quantitation of blood-brain barrier defect by magnetic resonance imaging and Gadolinium-DTPA in patients with multiple sclerosis and brain tumors. *Magn. Reson. Med.* 16:117-131; 1990.
- Tofts, P.S.; Berkowitz, B.A. Rapid measurement of capillary permeability using the early part of the dynamic Gd-DTPA MRI enhancement curve: Theory and validation. In: Book of abstracts: Eleventh Annual Meeting of the Society of Magnetic Resonance in Medicine, Vol. 1. Berkeley, CA:SMRM; 1992:868.
- Berkowitz, B.A.; Tofts, P.S.; Sen, H.A.; Ando, N.; de Juan, E. Accurate and precise measurement of blood-retinal barrier breakdown using dynamic Gd-DTPA MRI. *Invest. Ophthalmol. Vis. Sci.* 33:3500-3506; 1992.
- Larsson, H.B.W.; Tofts, P.S. Measurement of blood-brain barrier permeability using dynamic Gd-DTPA scanning—A comparison of methods. *Magn. Reson. Med.* 24:174-176; 1992.
- Tofts, P.S.; Berkowitz, B.A. Rapid measurement of capillary permeability using the early part of the dynamic Gd-DTPA MRI enhancement curve. *J. Magn. Reson.* 102:129-136; 1993.
- Kenny, J.; Schmiedl, U.; Maravilla, K.; Starr, F.; Graham, M.; Spence, A.; Nelson, J. Measurement of blood-brain barrier permeability in a tumour model using magnetic resonance imaging with gadolinium-DTPA. *Magn. Reson. Med.* 27:68-75; 1992.
- Wu, J.C.; Arrindell, E.L.; Wolf, M.D.; Nanda, S.K.; Han, D.P.; Wong, E.C.; Abrams, G.W.; Hyde, J.S. MRI evaluation of blood-retinal integrity following transconjunctival diode laser photocoagulation and retinal cryotherapy. In: Book of abstracts: Eleventh Annual Meeting of the Society of Magnetic Resonance in Medicine, Vol. 1. Berkeley, CA:SMRM; 1992:1515.
- Weinmann, H.J.; Laniado, M.; Mutzel, W. Pharmacokinetics of Gd-DTPA/dimeglumine after intravenous injection into healthy volunteers. *Phys. Chem. Phys. Med. NMR* 16:167; 1984.
- Tofts, P.S.; Shuter, B.; Pope, J.M. Ni-DTPA doped agarose gel—A phantom material for Gd-DTPA enhancement measurements. *Magn. Reson. Imaging* 11:125-133; 1993.
- Sato, Y.; Berkowitz, B.A.; Wilson, C.A.; de Juan, E. blood-retinal barrier breakdown caused by diode vs. argon laser endophotocoagulation. *Arch. Ophthalmol.* 110:277-281; 1992.
- Fenstermacher, J.D.; Blasberg, R.G.; Patlak, C.S. Methods for quantifying the transport of drugs across the brain barrier systems. *Pharmacol. Ther.* 14:217-248; 1981.
- Patlak, C.S.; Fenstermacher, J.D.; Blasberg, R.G. Graphical evaluation of blood-to-brain transfer constants from multiple-time uptake data. *J. Cereb. Blood Flow Metab.* 3:1-7; 1983.
- Blasberg, R.G.; Fenstermacher, J.D.; Patlak, C.S. Transport of  $\alpha$ -aminoisobutyric acid across brain capillary and cellular membranes. *J. Cereb. Blood Flow Metab.* 3:8-32; 1983.

25. Blasberg, R.G.; Patlak, C.S.; Fenstermacher, J.D. Selection of experimental conditions for the accurate determination of blood-brain transfer constants from single time experiments: A theoretical analysis. *J. Cereb. Blood Flow Metab.* 3:215-225; 1983.
26. Sondergaard, L.; Larsson, H.B.W.; Stubgaard, M.; Henriksen, O. The arterial concentration of Gd-DTPA can be monitored noninvasively. In: Book of abstracts: Eleventh Annual Meeting of the Society of Magnetic Resonance in Medicine, Vol. 1. Berkeley, CA:SMRM; 1992: 1120.
27. Edelman, R.R.; Mattle, H.P.; Atkinson, D.J.; Hill, T.; Finn, J.P.; Mayman, C.; Ronthal, M.; Hoggewoud, H.M.; Kleefield, J. Cerebral blood flow: Assessment with dynamic contrast-enhanced  $T_2^*$ -weighted MR imaging at 1.5 T. *Radiology* 176:211; 1990.